LA-14003

The Elusive Coefficients of Thermal Expansion in PBX 9502

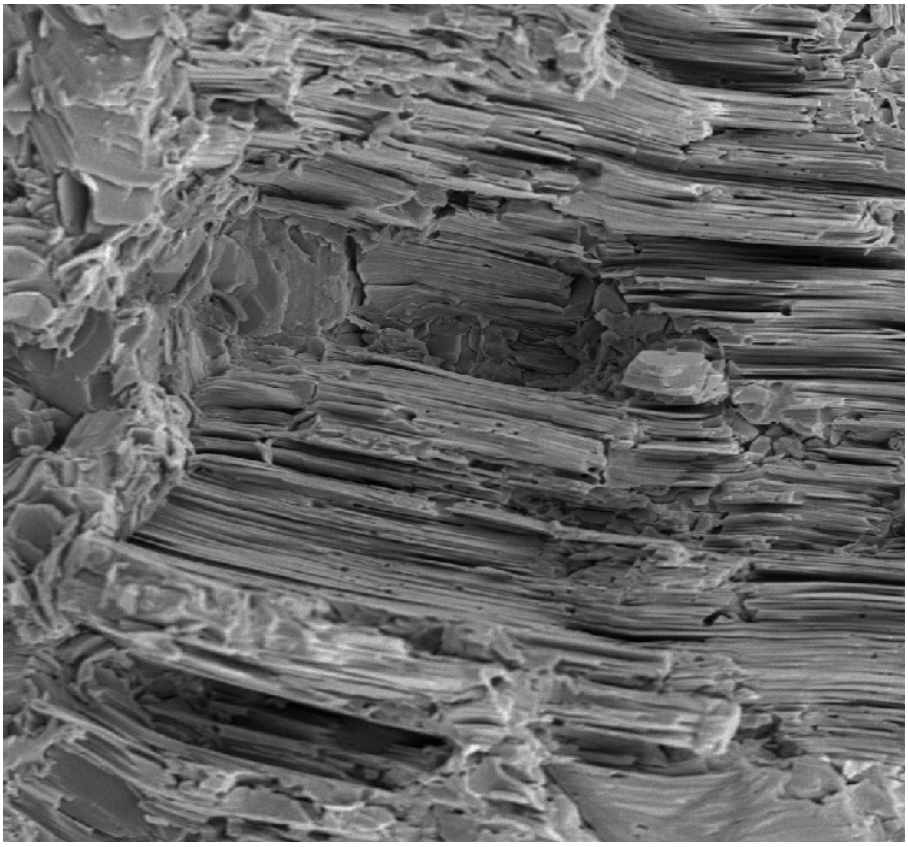

Los Alamos
NATIONAL LABORATORY

Editing by Belinda K. Haag, IM-1

Illustrations by J. Phil Putnam, IM-1

Cover Photo: Stacked sheets of TATB exposed by fracture in a consolidated PBX 9502 component.

Los Alamos National Laboratory, an affirmative action/
equal opportunity employer, is operated by the University
of California for the National Nuclear Security Administration
of the US Department of Energy under contract W-7405-ENG-36.

LA-14003
Issued: January 2003

The Elusive Coefficients of Thermal Expansion in PBX 9502

Cary B. Skidmore
Thomas A. Butler*
Cynthia W. Sandoval

*Consultant at Los Alamos, TechSource, Inc., P.O. Box 31057, Santa Fe, NM 87594-1057

Contents

List of Figures

List of Tables

The Elusive Coefficients of Thermal Expansion in PBX 9502

Cary B. Skidmore, Thomas A. Butler, and Cynthia W. Sandoval

Abstract

PBX 9502 has been in war reserve service for over two decades. Ninety-five percent of the solid phase of this insensitive high explosive is composed of energetic crystallites designated as TATB (1,3,5-triamino-2,4,6-trinitrobenzene), held together by the remaining solid fraction—an inert, polymeric binder named Kel-F 800. The unusual combination of extreme insensitivity and adequate performance characteristics is not the only enigmatic feature of such TATB-based materials. In this report, we describe the difficulty and progress to date in reliably determining the coefficients of thermal expansion for consolidated components of PBX 9502. We provide bulk linear coefficient of thermal expansion (CTE) values for PBX 9502 consolidated to a density of approximately 1.890 g/cm^3 and offer a simple set of equations for calculating dimensional changes for temperatures from 218 to 347 K (–55 °C to 74 °C).

1.0 Introduction

As computing power continues to grow, we can include more design details in models that simulate the response of complex systems to various stimuli. However, such details require more accurate material parameters. War reserve (WR) components of PBX 9502, an insensitive high explosive (IHE), are expected to help preserve system integrity while experiencing hot and cold temperature extremes. Understanding the CTE values for consolidated components of PBX 9502 is key to predicting thermal behavior during the components' service lives. While the thermal expansion parameters for TATB (single crystal, 1,3,5-triamino-2,4,6-trinitrobenzene) were well established over two decades ago (Ref. 1), the present state of knowledge for PBX 9502 is illustrated by comments from a recent report (Ref. 2):

> "For the stress analysis, the CTE for the PBX 9502 is very important. It was estimated based on collecting all available data and using an engineering judgement fit."

A CTE is simply a proportionality constant between a measured strain and the associated temperature change (Ref. 3). For experimental techniques that record changes in length, Eq. (1) applies:

$$\Delta L/L = \alpha_L \Delta T \,, \tag{1}$$

where

ΔL = change in specimen length,

L = original specimen length,

α_L = linear expansion coefficient, and

ΔT = temperature change that produced ΔL.

Table 1 provides CTEs of α_L for Al, Be, Cu, Fe, and Hg (Ref. 4) and for α-phase Pu (Ref. 5) at 25 °C.

Table 1. Coefficients for Linear Thermal Expansion in Various Metals

Element	α_L (µm/mK)
Al	23.1
Be	11.3
Cu	16.5
Fe	11.8
Hg	60.4
α-phase Pu	53.0

The corollary equation for volume is given in Eq. (2):

$$\Delta V/V = \alpha_V \Delta T \ , \tag{2}$$

where

ΔV = change in specimen volume,

V = original specimen length,

α_V = volumetric expansion coefficient, and

ΔT = temperature change that produced ΔV.

For isotropic materials, the volumetric CTE can be related to the linear CTE by Eq. (3):

$$\alpha_V = 3\alpha_L \ . \tag{3}$$

For some materials, such as graphite and mica, the thermal expansion varies with crystal direction (Ref. 3). A more general form of the equation for volumetric expansion is given in Eq. (4), where the subscripts *x*, *y*, and *z* correspond to coordinate directions in a bulk sample:

$$\alpha_V = \alpha_x + \alpha_y + \alpha_z \ . \tag{4}$$

The formula becomes more complicated at the single-crystal level for materials such as TATB. TATB is a member of the triclinic crystal system, which means the atoms are unequally spaced along three mutually oblique axes. The volumetric expansion therefore is not a linear combination of expansion along crystal axes.

1.1 Relevant Characteristics of Single-Crystal TATB

By mass and volume, TATB crystals are the principal solid-phase constituent (95%) in PBX 9502. The idiosyncrasies found in a single crystal of TATB influence the bulk behavior to a significant level in ways that are discussed later in our report. We lay the foundation here by reviewing the relevant characteristics of single crystals. The triclinic structure of TATB was firmly established by Cady and Larson (Ref. 6) using x-ray diffraction on a single crystal. Evidence was also reported for a very strong hydrogen bonding network (inter- and intra-molecular) within the *a-b* crystallographic plane. Such a bonding between the peripheries of planar molecules tends to form particles that are composed of layered sheets. Figure 1 is a secondary electron image from a scanning electron microscope (SEM) that shows a fracture surface in PBX 9502. The stack of sheets shown in the figure is similar to the edge view of a deck of playing cards. The crystallographic *c* axis is perpendicular to the sheets.

In the earliest written reference to CTEs for TATB (Ref. 7), Olinger and Cady determined the volumetric CTE (α_V) to be 99.5 $\mu m^3/m^3K$ by using a hot stage and a microscope to measure the change in dimensions of a single crystal over a 125-K temperature range. The only detectable expansion was perpendicular to the crystallographic *a-b* plane, or along the crystallographic *c* axis.

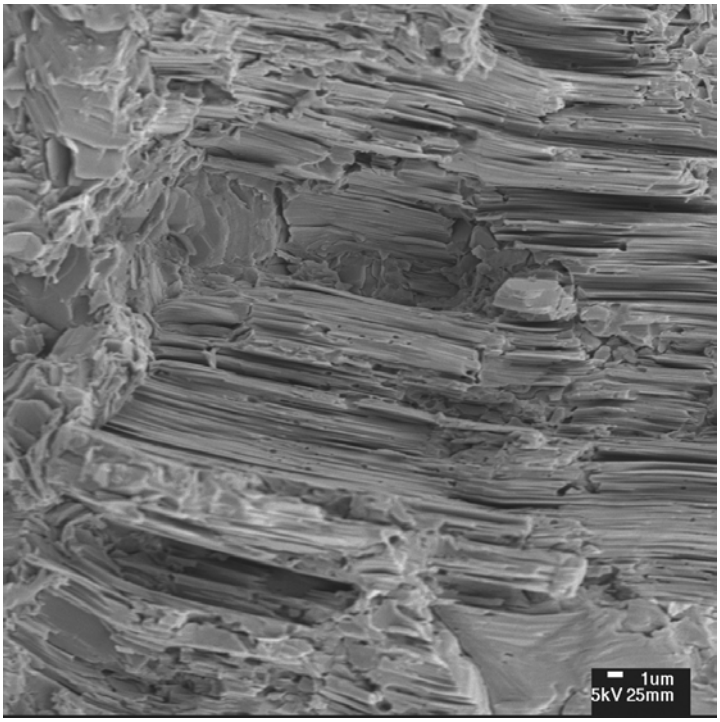

Fig. 1. Stacked sheets of TATB exposed by fracture in a consolidated PBX 9502 component.

A subsequent internal report (Ref. 8) corrected the value in deference to later results from a more accurate method reported by Kolb and Rizzo in Ref. 1 (304 $\mu m^3/m^3K$, 5.0% expansion).

Kolb and Rizzo used x-ray crystallography to measure a significantly larger average CTE in the *c* direction (248 μm/mK, 4.0% expansion) than in the *a* direction (8.3 μm/mK, 0.1% expansion) or *b* direction (20.9 μm/mK, 0.3% expansion) (over temperature range, 214–377 K). They attributed the enormous anisotropy to differences in bond strength: weak van der Waals forces in the *c* direction (between the layers) compared to the highly networked, stronger, hydrogen bonding within the *a*-*b* plane of the sheets.

Their work also showed that thermal expansion (in an isolated crystal) was completely reversible. There was no permanent growth even after temperature cycling. These results on a single, specially-prepared crystal (very slow recrystallization from hot nitrobenzene, unlike standard production synthesis used for WR powders), provide useful insight but cannot be applied directly to the bulk behavior of a consolidated PBX 9502 component, as we will demonstrate later in this report.

We note here that there are modest alterations to the chemical synthesis process that result in a different product. Cady (Refs. 9–10) and Rizzo et al. (Ref. 11) have described some of the microstructural differences in the resulting TATB crystals. The effect of intra-crystalline defects on thermal expansion, however, is unclear. The TATB used in the WR production of PBX 9502 is made by a process commonly referred to as “dry-amination.”

1.2 Effects of Consolidation

In practice, single crystals flocculate to form particles. If a group of TATB particles is compressed to form a consolidated article (compact), the thermal behavior of the bulk material is different from that expected by summing the response of individual particles. As early as 1979, Kolb and Rizzo (Ref. 1) reported average linear expansion coefficients (obtained using dilatometry) for "compacted polycrystallites" that were approximately half that expected, assuming that (1) the orientation of individual crystals is random and (2) the linear coefficient (α_L) is one-third the volume coefficient of expansion. By making an analogy with similar behavior observed in graphite, the difference was attributed to tensile microcracking in the compact.

In a subsequent report (Ref. 11), Rizzo et al. provided data to show that bulk CTE values in TATB compacts vary widely with the method of consolidation (pressing) and the median particle size. They obtained linear CTE data using a thermal mechanical analyzer, cooled the cylindrical samples to 223 K, and measured axial displacements as the samples were heated. Table 2 provides an extraction of their data, but we have substituted the terms "dry-aminated" and "wet-aminated" where they had listed normal TATB and chlorine-free TATB, respectively. Median particle size was determined by sieve analysis. The terms "isostatic" and "uniaxial" indicate the method of consolidation. We note that these data were collected on the sixth thermal cycle.

Table 2. Linear CTE Data from Ref. 11

Sample Description (TATB type, median particle size [µm], consolidation method)	Percent of Theoretical Maximum Density	Bulk Linear CTE (µm/mK) 223–263 K	Bulk Linear CTE (µm/mK) 313–343 K
Dry-aminated, 50, uniaxial	97.1	55	91
Dry-aminated (different lot), 50, isostatic	96.3	43	68
Wet-aminated , 100, uniaxial	97.7	95	150
Micronized wet-aminated, <10, uniaxial	97.3	110	142

Rizzo et al. (Ref. 11) also reported similar trends for identical temperature ranges in TATB formulated with 7.5 vol% Kel-F 800 binder. The uniaxially consolidated samples showed markedly higher values (62% for the lower range, 18% for the higher range) than the isostatically consolidated and machined samples, as measured by a thermal mechanical analyzer. Also, the lot with "fine particle size" dry-aminated TATB had an average bulk linear CTE which was 10% higher in the lower temperature range than the 50-µm dry-aminated TATB, as measured by dilatometry.

Rainbolt and Hatler (Ref. 12) reported "extremely high CTEs for pressed IHE" obtained with a steel-die uniaxial process compared to CTEs obtained with a semi-isostatic process to consolidate the material.

Edwards (Ref. 13) measured dimensional changes on hemispheres of PBX 9502 that were consolidated by two processes: hydrostatic and steel die. The hydrostatic process produced piece number 76-A39342-201 by employing the 3H press and the mold type MT A39, which has a 6.75-in. spherical outer radius and a 3.75-in. spherical inner radius. The steel-die process produced piece number 76-A34310-002, but no details of the mold dimensions are available. Flats were machined on each piece to facilitate gaging with calipers. A flat machined onto the pole was used to measure pole height and four flats machined around the equator were used to make two measurements of diameter. Dimensions were recorded at 225, 250, and 272.5 K (Table 3). We averaged the diametral values for each piece, used room temperature as a reference point for obtaining ΔT, and calculated the CTE. As a result, we observed the following trends:

1. In all cases, CTE increases with temperature.
2. The differences between consolidation methods are greater at higher T.
3. The steel-die pole height data is significantly greater than the hydrostatic pole height data. The diameter data are more similar to each other, which indicates that uniaxial consolidation produces compacts with more anisotropy.

Table 3. Average Linear CTE for PBX 9502 Hemispheres Consolidated by Hydrostatic and Steel-Die Processes

Temperature (K/°C)	Average Linear CTE (µm/mK)			
	Diameter Hydrostatic	Diameter Steel Die	Pole Height Hydrostatic	Pole Height Steel Die
225/–48	40.8	39.2	37.3	50.8
250/–23	42.1	40.3	40.5	55.9
272.5/–0.5	48.9	43.9	44.0	65.2

Cady (Ref. 14) measured CTEs at 233, 293, and 333 K on cubes cut from a hemispherical shell. Semi-isostatic consolidation was accomplished by isostatically pressing PBX 9502 molding powder against a hemispherical mandrel (Fig. 2). Cubes were cut along three different radial lines to obtain a total of 12 cubes. For half of the cubes, Cady measured linear expansion along a radial direction, and for the other half, he measured expansion parallel to a line tangent to the outer surface of the hemispherical shell. In his analysis, Cady observed that expansion was 16–19% greater in the radial direction than in the tangential direction (Table 4). The radial direction in a semi-isostatic consolidation is analogous to the axial direction in a uniaxial process.

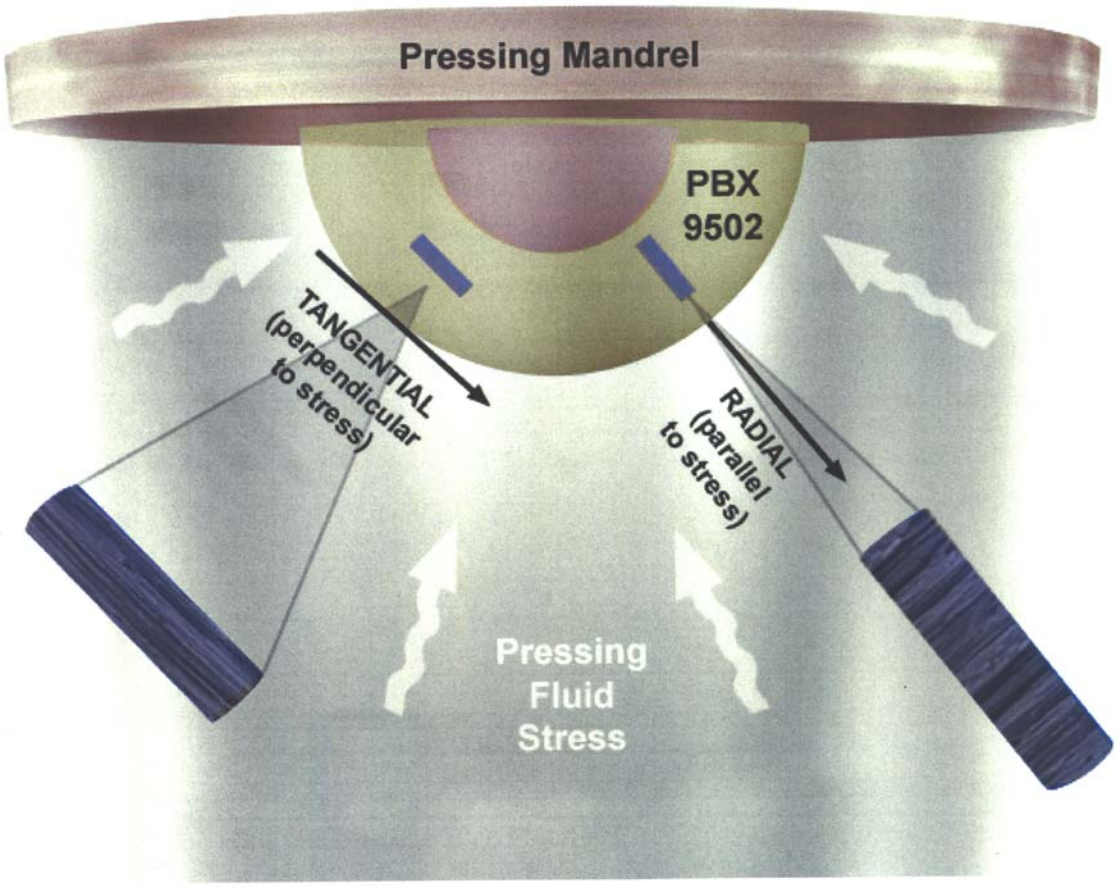

Fig. 2. Schematic diagram of the semi-isostatic consolidation process.

Table 4. Linear CTE Data from Ref. 14 for Specimens from a Hemispherical Sample

Temperature (K/°C)	Linear CTE (μm/mK)	
	Tangential	Radial
233/–40	42	50
293/20	56	66
333/60	73	84

Maienschein and Garcia (Ref. 15) conducted thermal expansion experiments on a composition that incorporates 92.5 wt% wet-aminated TATB (LX-17-1) over the temperature range 300–566 K. They report these two effects in uniaxially-compacted cylinders:

- Hot-pressed (375 K) samples show more expansion than cold-pressed (room temperature) samples.
- Expansion in the axial direction was 1.4 to 1.7 times greater than in the radial direction.

Kolb, Rizzo, Cady, and Maienschein all attribute the CTE anisotropy observed in compacts of TATB or TATB-based explosives to an ordering of some fraction of the TATB crystals during the consolidation process.

Apparently, the *a*-*b* crystal plane tends to orient itself perpendicular to the direction of applied pressure. Or, in other words, the *c* axis, which has the highest CTE by an order of magnitude, aligns with the principal applied stress. If a sufficient number of individual crystals in a compact are randomly oriented, the assumption is that bulk linear CTE is one third of the volumetric CTE. If the number is insufficient, the assumption becomes invalid. Therefore, a bulk linear CTE value may not be adequate for engineering designs involving PBX 9502 components, particularly where there are close-tolerance interfaces with components made from other materials having significantly different CTEs. We also note that any attempt to measure the CTE values in a PBX 9502 compact must consider the details of the consolidation process, including the orientation of the compact with respect to the direction of the principal applied stress.

Cady conducted x-ray diffraction (XRD) experiments on uniaxially pressed cylinders (50 mm diam. × 25 mm height, density of 1.870 g/cm^3) of X-0219 (an early TATB explosive) (Ref. 16). He concluded that 19% more of the crystallites were oriented with their planes perpendicular to the direction of the principal applied stress than would be the case for a sample with 100% random orientation of the crystallites. This observation of pressing-induced texture was qualitatively confirmed in XRD experiments conducted by Phillips (Ref. 17) on PBX 9502.

1.3 Irreversible Growth

Another complication in determining CTE values for compacts of PBX 9502 is the phenomenon of irreversible or “ratchet” growth that occurs with temperature cycling in an unconfined state. This phenomenon does not occur in single crystals of TATB but is a complex product of the microstructural interactions of particles with each other and with binder (if present). The topic of ratchet growth is worthy of its own investigation and report. We describe “growth” in our report only to distinguish it from “expansion” and to describe how to avoid it in CTE experiments.

Ratchet growth is simply the explanation for a significant difference in dimensional measurements before and after temperature cycling (hysteresis). Rizzo et al. (Ref. 11)

reported that "repeated thermal cycling between –54 and 74 °C of high density, pure and plastic-bonded TATB billets causes a permanent volume expansion (growth) of about 1.5 to 2.0 vol%." Mulford and Romero (Ref. 18) reported an average permanent volume expansion of 3.24% in 10 machined cylinders of PBX 9502 (2 in. × 2 in.) which were heated from room temperature to >200 °C for at least five cycles.

Thermal expansion is a lattice stretch and is expected to produce higher-level stresses than those generated by the growth mechanism. Flaugh (Ref. 19) reported that "irreversible growth is eliminated if PBX 9502 is maintained at a pressure of 60 psi." Cady (Ref. 14) cited unpublished work by Manuel Urizar that concluded that irreversible growth is a low-stress phenomenon that can be prevented by pre-loading the piece to 50 psi. Rizzo et al. (Ref. 11) concluded that "the growth of TATB with 10 vol% Kel-F 800 is reduced from 5 to 2 mm/m when a force of 552 kPa (80 psi) is applied." They also referenced experiments with cylinders (10% binder) that are confined on all surfaces except one axial face and heated at 120 °C for one to four months. The entire volume increase (1.5%) was manifested as growth in the axial direction.

To provide for a simpler configuration and in order to obtain the maximum value (worst-case), we choose to make our thermal expansion measurements on unconfined samples. System designs based upon these values must then assume that the values are not appreciably affected, or at least not adversely affected, by anticipated levels of confinement.

We recommend that the CTE experimenter take the following precautions in order to minimize the influence of the growth mechanism:

- Temperature cycling should be considered to alter the original condition of the specimen.
  - Replications should be performed on separate specimens, not by repeating a temperature sequence on any one specimen.
  - If a specimen run meets with technical difficulty, the specimen should be replaced before the run is repeated.
- The "return" portion of data that exhibits hysteresis should be considered invalid with respect to CTE.

1.4 History of CTE Measurements for PBX 9502

When Kolb and Rizzo were publishing detailed results from CTE experiments on single-crystal TATB, researchers and engineers were struggling to define CTE parameters for the PBX compositions. Consider the following comments in 1979 from Flaugh (Ref. 19):

> "We have had continual problems measuring the CTE of plastic bonded TATB. Initially, irreversible growth and TATB crystal orientation confused the CTE measurements…. We have generated CTE numbers from 32 to 90 × 10^{-6}/°C for various batches of PBX 9502, not exactly reassuring precision. In an attempt to discover the real CTE for PBX 9502, … but there is still considerable variability between lots of PBX 9502 powder."

Flaugh described an effort to separate the irreversible growth from CTE by "conditioning" the PBX 9502 before making the CTE measurements. Test pieces were cycled at least 20 times between the temperature extremes of 219 K and 347 K "to essentially eliminate irreversible growth." After making CTE measurements on a number of samples, a value of 62 μm/mK was chosen to represent the entire temperature range.

After that work, Flaugh obtained lower values using "standard mechanical measurements" and a density technique (piece densities were measured at the temperature extremes and converted to an "effective linear CTE"). He concluded by recommending that two values should be used for the linear CTE of PBX 9502, each corresponding to a different temperature range (38 μm/mK for 219–303 K and 50 μm/mK for 303–347 K).

In 1998, Rainbolt and Hatler (Ref. 12) stated that "the issue of what coefficient of thermal expansion value is correct for PBX 9502 has been discussed in various meetings and initiated a review of the existing data." They derived a formula based upon experimental data using five parts taken from PBX 9502 hemispherical shells consolidated in an semi-isostatic process. The temperature ranged from 219 to 303 K. The authors recommended "using the formula to calculate the CTE in future structural and thermal models." The formula is

$$CTE_T = (42.33 + 0.212T)\ \mu m/m°C\ , \tag{5}$$

where T is the temperature in degrees Celsius. We note that this is a straight-line approximation.

Performance characteristics of PBX 9502 at various temperatures have been studied in several experiments. In some configurations, the thermal expansion of PBX 9502 was considered an important parameter, and CTE data were reported. In 1984, Campbell (Ref. 20) conducted rate-stick experiments to measure diameter effects on the steady detonation of PBX 9502 at temperatures of 218 K (–55 °C), 297 K (24 °C), and 348 K (75 °C). He reported the thermal expansion along the axis of a stack of right circular cylinders. Each cylinder, or segment, was 50 mm long and the diameter varied from 5.7 mm to 50 mm. A typical stack contained eight segments, all of the same diameter. The average density for all segments in a stack varied from 1.887 to 1.894 g/cm^3 for the 15 experiments in which thermal expansion was measured. The consolidation method used in Campbell's work was not specified. The axial load for the assembly was 700 g/cm^2 (10 psi). Using 297 K as the reference point and dial indicators to detect displacement, he reported that expansion at the cold extreme (218 K) ranged from 52–60 μm/mK (average α_L = 56 μm/mK for seven experiments) and the expansion at the hot extreme (348 K) ranged from 66–89 μm/mK (average α_L = 79 μm/mK for eight experiments). There was no apparent correlation of density extrema with α_L extrema.

In 1998, Hill et al. (Ref. 21) conducted a similar study with more attention to the anisotropic nature of the thermal expansion. Segments were consolidated by a nominally isostatic method to a density of 1.890 ± 0.005 g/cm^3. Segment diameters were nominally 10, 18, or 50 mm at the reference temperature of 298 K (25 °C). The cylindrical stack was spring loaded along the axis and centering rings at each joint touched the diameter at three points.

Dial indicators were used to detect displacements along the axis and one radius location. Data appearing in Table 1 of Hill's report are listed in Table 5 below. The mean CTE values represent three experiments each. In his report, Hill commented, "When tested on inert reference materials, the thermal expansion gauges produced handbook values. The same measurements performed on PBX 9502 were somewhat erratic." This result is largely attributed to specimens cored from various locations in a heterogeneous billet. The PBX 9502 used in these experiments was taken from lot HOL88H891-008, which contained 50% recycled material.

Table 5. Mean CTE Data from Ref. 21 for Cylinders

Temperature (K/°C)	Mean CTE (µm/mK)			
	Axial (α_A)	Radial (α_R)	Volumetric ($\alpha_V = \alpha_A + 2\alpha_R$)	Nominal Linear ($\alpha_L = \alpha_V/3$)
218/–55	64	39	142	47
348/75	125	68	261	87

2.0 Experiments

Currently there is no specification of acceptable range for CTEs for PBX 9502 WR components, and there is no direct surveillance of this material property. However, thermal expansion could be considered as an integrated response of all the microstructural elements present in a specimen (e.g., crystallites, intracrystalline voids, binder adhesion, polymer molecular weight, and interparticle pores) just as much as tensile or compressive strength is considered to be an integrated response of those elements. Parameters that are important in mechanical properties testing may also be important considerations in measuring CTE.

In designing our experiment matrix, we considered knowledge gained from recent mechanical properties testing and from past CTE research. We wanted to establish a baseline with non-WR material and then examine stockpile returns. Parameters were prioritized in order to reduce the scope of the study. To make the measurements, we used a Harrop Industries® thermodilatometric analyzer (Model TD-720-C), which has a reported sensitivity of less than 0.00001 in. (0.254 µm).

Our first priority was to measure α_L for specimens machined from a freshly pressed cylinder (semi-isostatic method, 9.75 in. diameter and 5 in. height) using a nominal lot of PBX 9502 (HOL80H890-006). Specimens were cored from the mother derby into cylinders measuring 0.375 in. diameter and either 1 or 2 in. long. Ten specimens were cored with the specimen axis parallel to the axis of the mother derby and 10 were cored with the specimen axis perpendicular to the axis of the mother derby. Figure 3 shows the orientation of the specimens with respect to the mother derby. Five from each set were 1 in. long and the remaining five were 2 in. long. Immersion densities varied from 1.886 to 1.890 g/cm^3 with an average of 1.889 g/cm^3 and a standard deviation of 0.001 g/cm^3. Other specimens (all 1-in. long) have been machined but have not yet been tested. Table 6 summarizes all the specimens that have been prepared for our study.

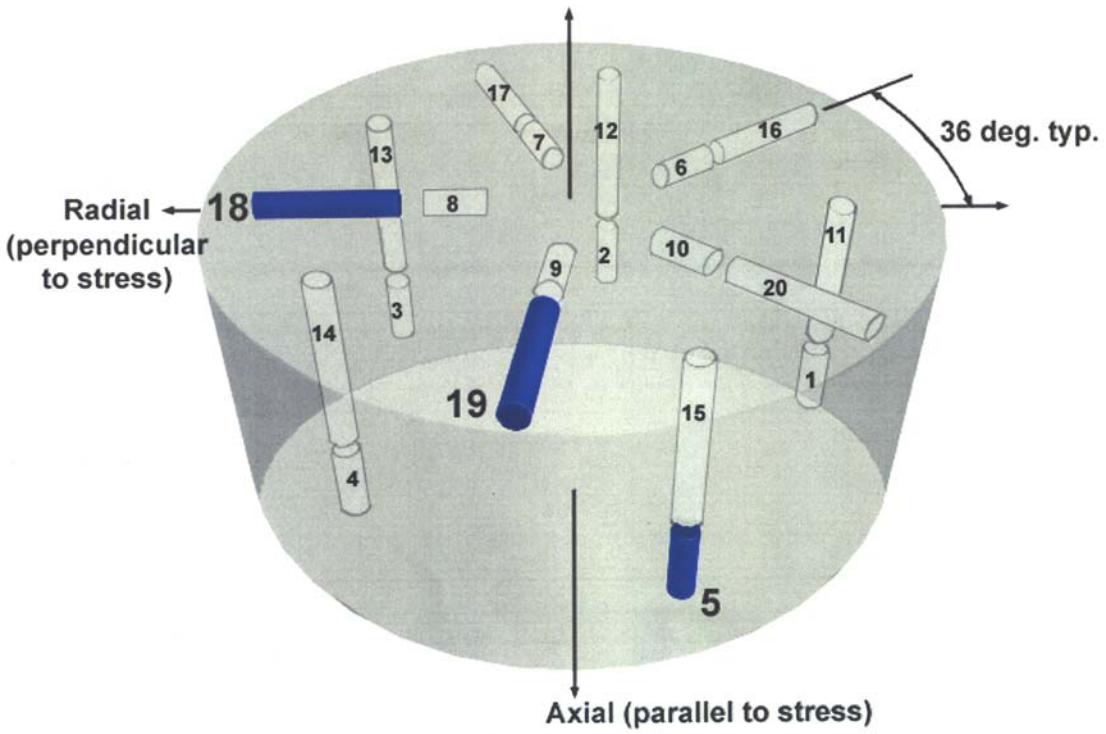

Fig. 3. Transparent model that shows the orientation of specimens with respect to the mother derby.

We used a linear variable displacement transducer (LVDT) to measure the change in length. Heating was accomplished using radiance from an electrical resistance source. Cooling was accomplished by dispensing head vapor from a liquid nitrogen Dewar as dictated by a programmed process controller. Each specimen was held in a temperature soak at 298 K (25 °C) for 5 min. The temperature was programmed for a ramp rate of 2 K/min. with an LVDT displacement recorded approximately every 30 s. One complete cycle was executed between the nominal temperature extremes of 218 K (–55 °C) and 358 K (85 °C). The sequencing in the cycle was varied as part of the study: sometimes the specimen was heated first and sometimes it was cooled first. The initial temperature was experienced three times. For example, a heat-first sequence followed this pattern: soak at 298 K, heat to 358 K, cool to 218 K; the specimen would then pass through the initial temperature for the second time, then heat to 298 K.

Table 6. Summary of PBX 9502 Specimens

PBX 9502 Molding Powder Lot	Parent Piece	Specimens			Status
		Number	Orientation	Length (in.)	
HOL80H890-006	99-B04035-0001	5	Parallel	1	Tested
		5	Perpendicular	1	Tested
		5	Parallel	2	Tested
		5	Perpendicular	2	Tested
HOL86A891-004 (50% recycle)	98-418341-0001	5	Parallel	1	Pending
		5	Perpendicular	1	Pending
	98-418344-0001	5	Parallel	1	Pending
		5	Perpendicular	1	Pending
HOL83M890-021	802070529	5	Radial	1	Pending
		5	Tangential (Equatorial)	1	Pending
	WR Return	5	Radial	1	Pending
		10	Tangential (Polar)	1	Pending
HOL85H891-003 (50% recycle)	802110748	5	Radial	1	Pending
		5	Tangential (Equatorial)	1	Pending
	WR Return	5	Radial	1	Pending
		10	Tangential (Polar)	1	Pending

In our thermal analysis, we used ABAQUS (Ref. 22) to estimate the time necessary for a specimen to change temperature. For this analysis, we used the following parameters for PBX 9502:

- Density: 1.890 g/cm^3
- Thermal conductivity: 0.55 W/mK (1.32×10^{-4} cal/s/min.)
- Specific heat: 900 J/kgK (215 cal/kgK)
- Convection coefficient: 10 (this number is based on typical convection for unforced air in a room or natural convection in still air)

The model showed a steady-state temperature difference of 0.62 K between the core and surface when the atmosphere T was changed at the rate of ~2 K/min. This calculation of the time constant shows that the heating rate seems to be appropriate.

Our experience with the instrument and analysis of the data from the 20 specimens from lot HOL80H890-006 will guide the procedure for future experiments. The next set will measure the CTE for specimens from a 50% recycle lot of PBX 9502 (HOL86A891-004). Specimens from this lot (0.375 in. diameter, 1 in. length) have been cored from two mother derbies (semi-isostatic method, ~9 in. diameter, 6 in. height). Five specimens were cored from each derby with the specimen axis parallel to the axis of the mother derby and five were cored with the specimen axis perpendicular to the axis of the mother derby.

Two similar sets of specimens have been prepared using PBX 9502 lots returned from stockpile service: one that is 50% recycle material (HOL85H891-003) and one that is not (HOL83M890-021). In this case, however, parallel corresponds to radial and perpendicular to tangential.

2.1 Results

Thermocouple data from typical heat-first and cool-first sequences for specimens 4 and 5 are shown in Fig. 4. The greater waviness during the cooling stages is typical and probably indicates more difficulty in controlling the cooling process. Figure 5 shows corresponding LVDT displacements for specimens 4 and 5. The messy data near ambient temperature is typical and may have been influenced by a glass transition temperature (Tg) range near ambient (Ref. 23).

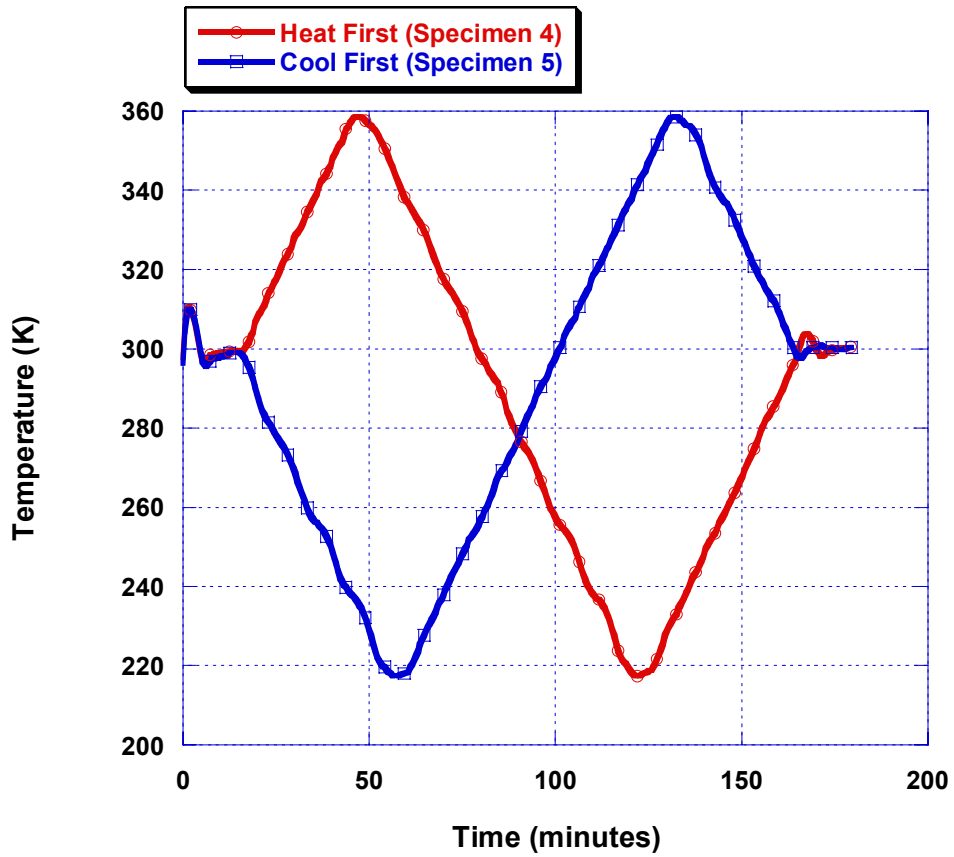

Fig. 4. Typical heat-first and cool-first sequences.

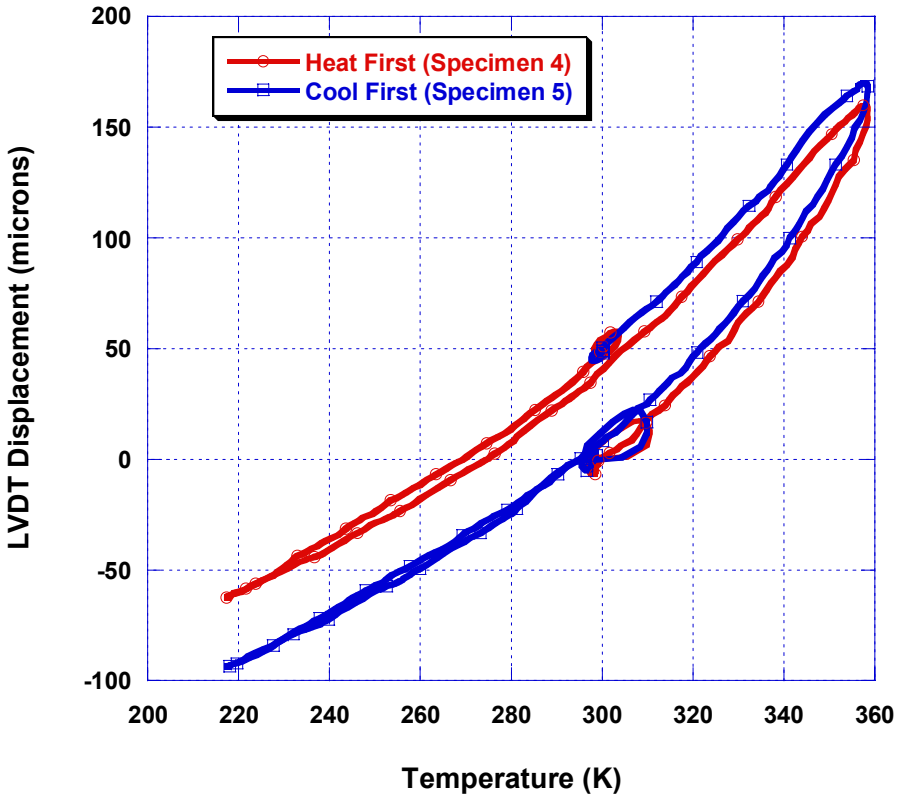

Fig. 5. Typical pattern for LVDT displacement.

The data show a significant discrepancy in LVDT displacement between the start and end of the cycle. We attribute the discrepancy to irreversible growth and note that it is more prevalent after passing through the hot temperature extreme than the cold. For several of the specimens, problems with the initial run required a rerun. These are noted in the Comments column of Table 7. We note that the values for original specimen lengths shown in Table 7 are consistently higher for the retested specimens. For the 2-in. long specimens, half were retested. Their average initial length was 100 µm greater than the average initial length (with a standard deviation of only 5 µm) for the specimens tested only once. This provides additional evidence of irreversible growth from the first test. Many of the runs had an initial spike of high temperature (16 out of 20 or 80%), which is noted in the Comments column of Table 7.

Table 7. Tested Specimens

Specimen Number	Test Label	Temperature Sequence	Specimen Orientation	Original Specimen Length, L_0 (m)	Comments
1	#1par1H	heat first	parallel	0.02539	Initial spike to 310 K
2*	#2par1-2C	cool first	parallel	0.02540	Initial spike to 315 K, data for rerun only
3	#3par1H	heat first	parallel	0.02541	Initial spike to 309 K
4	#4par1H	heat first	parallel	0.02541	Initial spike to 311 K
5*	#5par1C	cool first	parallel	0.02540	Initial spike to 310 K
6	#6per1C	cool first	perpendicular	0.02541	Initially 320 K for 5 min 223 < Temp (K) < 367
7	#7per1-2H	heat first	perpendicular	0.02543	Data for rerun only
8	#8per1-2H	heat first	perpendicular	0.02541	Data for rerun only
9*	#9per1C	cool first	perpendicular	0.02539	Initial spike to 311 K
10*	#10per1-2C	cool first	perpendicular	0.02542	Initial spike to 309 K, data for rerun only
11	#1par2-2H	heat first	parallel	0.05100	Initial spike to 307 K, data for rerun only
12	#2par2-2H	heat first	parallel	0.05094	Data for rerun only
13	#3par2H	heat first	parallel	0.05079	Initial spike to 311 K
14*	#4par2-2C	cool first	parallel	0.05083	Initial spike to 309 K, data for rerun only
15*	#5par2-2C	cool first	parallel	0.05082	Initial spike to 311 K, data for rerun only
16	#6per2-2C	heat first	perpendicular	0.05090	Initial spike to 313 K, data for rerun only
17	#7per2H	heat first	perpendicular	0.05080	Initial spike to 311 K
18*	#8per2C	cool first	perpendicular	0.05080	Initial spike to 308 K
19*	#9per2C	cool first	perpendicular	0.05079	No initial spike
20	#10per2H	heat first	perpendicular	0.05080	Initial spike to 307 K

*The eight specimens discussed in the analysis.

2.2 Analysis

Up to this point, we have stated temperatures in units of Kelvin. In order to make the results more user friendly to the general engineering community, we will state temperatures in degrees Celsius for the remainder of the report. We also acknowledge that we have used CTE units, μm/mK, in order to avoid repetitive use of the somewhat unwieldy exponential term. Subsequent plots and equations herein provide a CTE value that includes the traditional exponential term.

We analyzed only the data from the cool-first runs and, in addition, only the data that represented one continuous span from cold to hot. Limiting the data in this manner minimized the effects of ratchet growth. These criteria eliminated all but nine runs from the test set. Of these nine runs, specimen 6 did not span the complete temperature range so it was also eliminated, therefore resulting in eight runs that we used in our initial analysis. In Table 7, these runs are designated with an asterisk next to the specimen number.

Normalized LVDT displacement data are plotted as a function of temperature in Fig. 6 for the eight runs analyzed. From this point forward, the data are limited to a temperature range of interest from –55 to 74 °C (218 to 347 K). We observe that for PBX 9502, the displacement increases non-linearly with temperature. While we did not measure posttest specimen density, this displacement trend is consistent with the non-linear decrease in density reported by Dallman et al. (Ref. 24) over the same temperature range. Before proceeding with further analysis, the displacement data were fit with a fourth-order polynomial for each specimen.

The derivative of the displacement fit yields the instantaneous CTE. This value is shown for all eight specimens in Fig. 7. The curves fall naturally into three groupings. The differences between them increase with temperature. The grouping with the highest CTE is composed of data for specimens 14 and 15. Their fits are very similar and lie distinctly above the others. Both of these specimens have the parallel orientation and data for both were collected on the second heating of the material.

The grouping with the mid-range CTE values is composed of data from specimens 2, 5, 18, and 19. Specimens 2 and 5 have the parallel orientation while specimens 18 and 19 have the perpendicular orientation. Within this grouping, only specimen 2 data were collected by retesting.

The grouping with the lowest CTE values is composed of data from specimens 9 and 10 (perpendicular orientation). Comparing CTE values within a grouping, these are the most disparate. The CTE values for specimen 9 are distinctly lower than those for specimen 10, which were collected during retesting. These specimens are very similar in every other observable characteristic.

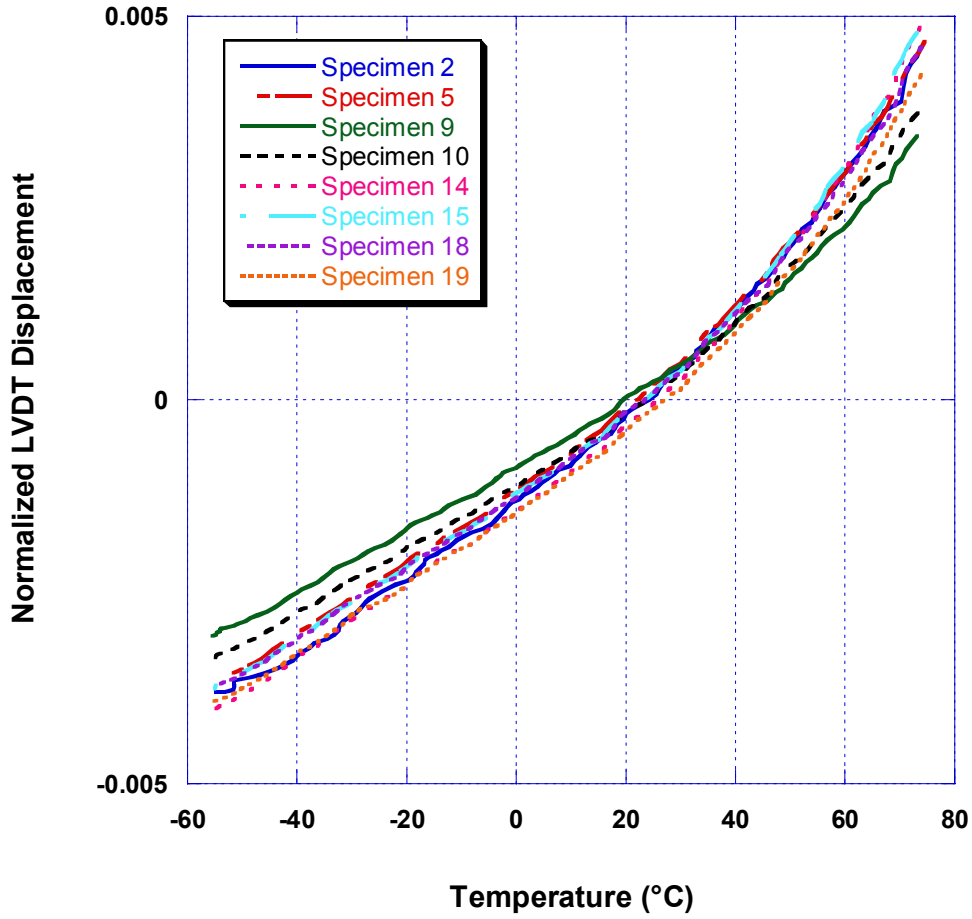

Fig. 6. Normalized LVDT displacement for eight specimens.

From these observations, we first consider the effect of retesting on CTE values. As previously mentioned, our results (Fig. 5) show that heating produces irreversible growth. We also noted earlier the significant difference in average original length for tested and retested 2-in. specimens. We would expect a similar trend in the 1-in. specimens of about half the magnitude, or 50 µm, but it is not present. This result could be because the retested specimens were never heated during the aborted first tests, or the value for original specimen length was retained from the first test rather than making a new measurement. Half of the retested 1-in. specimens were intended to be heat-first tests, so it seems that they would have been heated to some higher temperature, experienced some growth, and resulted in a larger L_0 than is recorded. If so, the true L_0 is larger than the value used to calculate the normalized LVDT and the displacement data is erroneously inflated. This would cause the CTE curve for specimen 2 to be higher than that for specimen 5 (comparing the parallel, 1-in. specimens), and the curve for specimen 10 to be higher than that for specimen 9 for the perpendicular specimens. This is clearly the case for the latter pair, but not the former pair. Our retesting of specimens introduced significant ambiguity and clouded the interpretation of the data.

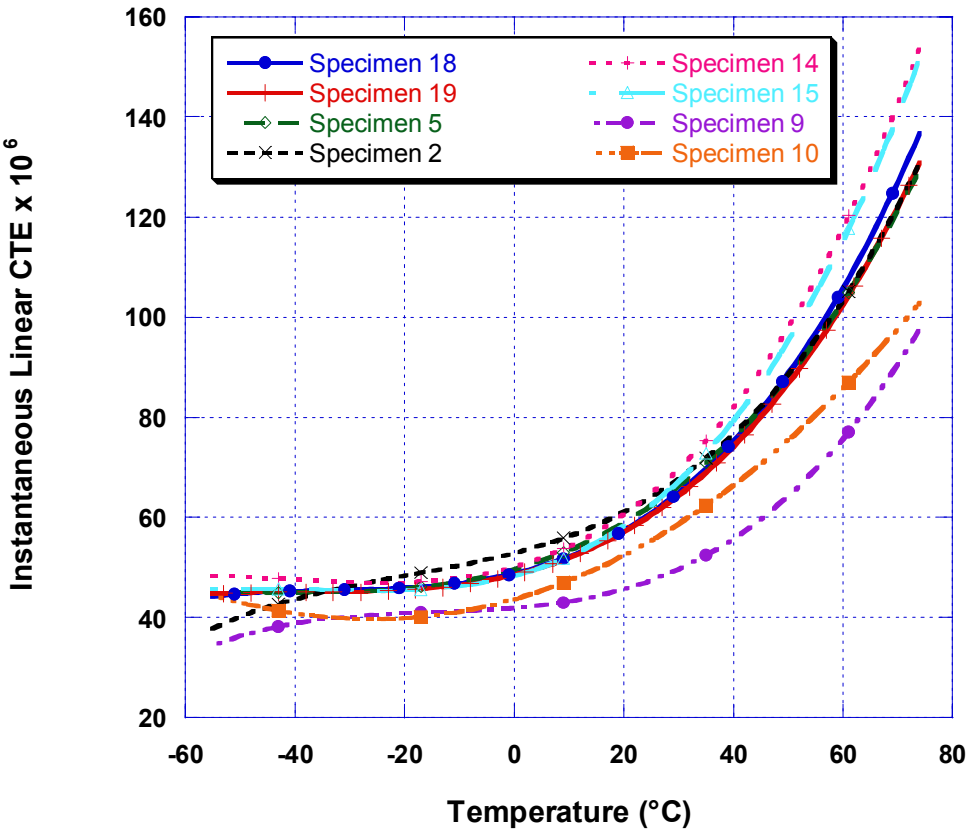

Fig. 7. Instantaneous linear CTE curves for eight specimens.

In order to avoid confusion, we argue that the hysteresis exhibited by the material after the first heating cycle indicates that the material has been altered. Our purpose is to determine the CTE of unaltered material; therefore, we omit from our analysis the CTE data from any of the specimens that were retested. Subsequently, we consider data from specimens 5, 9, 18, and 19.

For these specimens, we consider the effect of specimen orientation with respect to the pressing direction and location from within the mother derby. Specimen 5 is the only one of the four with a parallel orientation and its CTE data are within the same grouping as that for the perpendicular specimens 18 and 19. Therefore, from these very limited data we must conclude that there are no orientation effects. If we had valid data from 20 specimens, perhaps our conclusion would be different.

In order to understand why the data for specimen 9 do not fit with the data from the other three specimens, we analyzed the density data and discovered that there is a statistically significant difference between them. The measured density of specimen 9 was 1.8876 g/cm^3, while the average density of the final set was 1.8899 g/cm^3 with a standard deviation of 0.0003 g/cm^3, resulting in a minimum difference of 0.002 g/cm^3. While a conclusive study on the effect of density on CTE has not yet been reported, we suggest that perhaps the lower density of specimen 9 produced the lower CTE observed. We also note that specimen 9 came from the center of the mother derby, whereas the other three specimens came from the outer

region (Fig. 3) and may have been consolidated differently. As mentioned previously, Hill (Ref. 21) attributed erratic results for CTE in PBX 9502 to pressing-induced heterogeneities in the original billet. Therefore, we consider specimen 9 to be of somewhat anomalous origin and omit it from further consideration.

The instantaneous CTE curves for the final three specimens are isolated in Fig. 8 prior to proceeding with their conversion to secant CTE curves. Equation (6) shows the average of the three curves (with standard deviations). Values for T are given in degrees Celsius.

$$CTE_{instantaneous} = 4.90 \pm 0.06 \times 10^{-5} + 2.78 \pm 0.27 \times 10^{-7} T + 6.97 \pm 0.19 \times 10^{-9} T^2 + 6.09 \pm 1.20 \times 10^{-11} T^3. \quad (6)$$

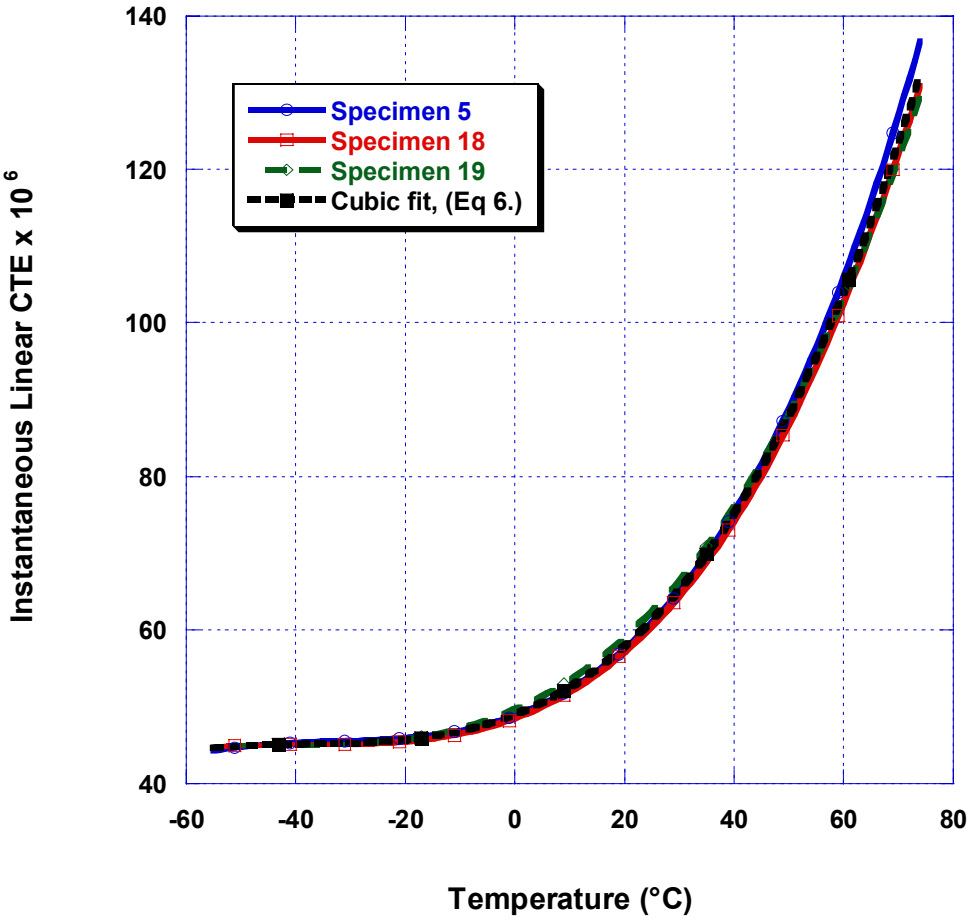

Fig. 8. Instantaneous linear CTE for the three specimens selected for final analysis.

A secant-based CTE is often of more practical use in engineering calculations and materials models. When considered as a set, the secant CTE from specimens 5, 18, and 19 can be fit with the following cubic equation (with standard deviations), where T has the units of degrees Celsius.

$$CTE_{secant} = 5.31 \pm 0.07 \times 10^{-5} + 1.94 \pm 0.09 \times 10^{-7} T + 2.64 \pm 0.10 \times 10^{-9} T^2 + 1.83 \pm 0.24 \times 10^{-11} T^3 \cdot \quad (7)$$

The reference temperature for Eq. (7) is 21 °C. The secant CTE for each of the three runs with the final fit are shown in Fig. 9.

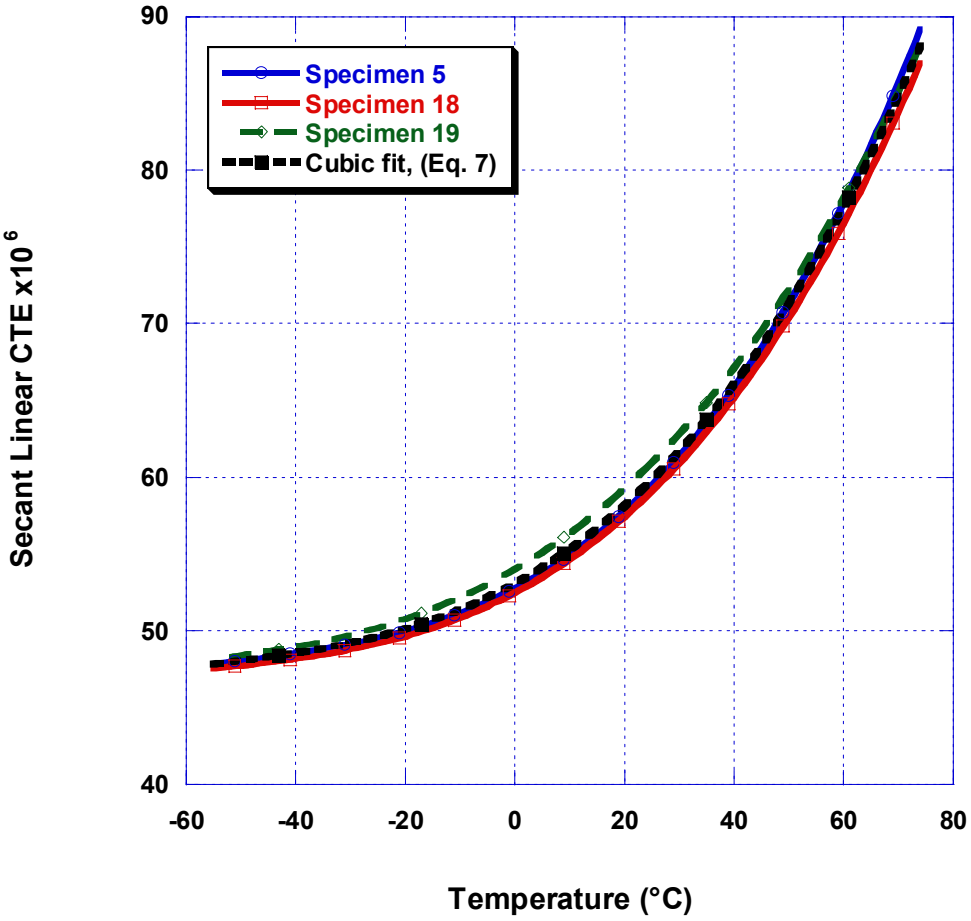

Fig. 9. Secant linear CTE for the three specimens and their cubic fit.

2.3 Discussion

In order to avoid misapplication of our CTE data in calculating thermal growth or in making comparisons to other CTE data, we provide the following discussion. We first remind the reader that differences in consolidation method, density, or lot-specific characteristics such as particle size can affect the accuracy of the calculation. We also note that the possible effect of confinement on the thermal growth of the specimen was not investigated. All our work is reported for the unconfined state.

We review here the differences between a secant CTE and an instantaneous CTE in application. The secant and instantaneous methods each provide an equally accurate final dimension when properly applied. The secant approach offers the simplest case, so we present it first. We assume that the initial value for a linear dimension, L_{ref}, is known at the secant reference temperature, T_{ref} (i.e., 21 °C), and that the value, L_f, for the same dimension at a different, final temperature, T_f, is desired. After using Eq. (7) to calculate CTE_{secant} at T_f, Eq. (8) may be applied. Equation (8) is simply a rearrangement of Eq. (1) after expanding the delta terms.

$$L_f = L_{ref} [1 + CTE_{secant} (T_f - T_{ref})] . \quad (8)$$

This process seems straightforward. However, we wish to emphasize the absolute necessity of using the secant version of the CTE in this equation when working with PBX 9502. For common structural metals, the CTE is nearly constant for most normal environments and this distinction is not necessary. For literature references on CTE of TATB-based materials, it is not always clear whether the reported values are derived from a secant approach or an instantaneous method. However, our work has shown that the CTE value at a given temperature is quite different on the instantaneous data curves compared to the secant fit curve. For example, consider the CTE values for specimen 19 at 60 °C. The secant CTE is 78 μm/mC while the instantaneous CTE is 103 μm/mC. Using the wrong CTE value could lead to the wrong conclusion in some applications.

If the initial value for a linear dimension, L_0, is known at a temperature, T_0, that is not the secant reference temperature, T_{ref} = 21 °C, a simple modification of Eq. (8) is required. After using Eq. (7) to calculate the secant CTE at both the initial and final temperatures, Eq. (9) may be applied:

$$L_f = L_0 [1 + CTE_{secant0} (T_{ref} - T_0) + CTE_{secantf} (T_f - T_{ref})] . \quad (9)$$

In the secant approach, the final length change can be thought of as the vector resulting from the addition of the vector from the initial condition to the reference point and the vector from the reference point to the end condition.

For the instantaneous approach, the CTE value represents the derivative of normalized length change with respect to temperature. The calculation of length change between two temperatures requires integration. Practically speaking, this means that we must calculate and sum the incremental growth for each step change from the initial temperature to the final

temperature, using the CTE values from the instantaneous curve at each temperature along the way.

In order to compare the experimentally determined CTE values of various researchers, we must know which data type has been reported and compare only similar types. In Fig. 10, we compare our cubic fit for secant CTE values with data from other LANL researchers. Because these data were reported for only a few discrete and widely separated temperatures that do not provide a continuous curve, we have assumed them to be secant CTE values. As explained previously, the radial direction for a semi-isostatically pressed hemisphere is analogous to the axial direction for a cylinder because both are parallel to the pressing force. Likewise, the tangential direction in a hemisphere is analogous to the radial direction in a cylinder because both are perpendicular to the pressing force. For greater clarity in comparison, we use only the designations “parallel” and “perpendicular” in the legend of Fig. 10.

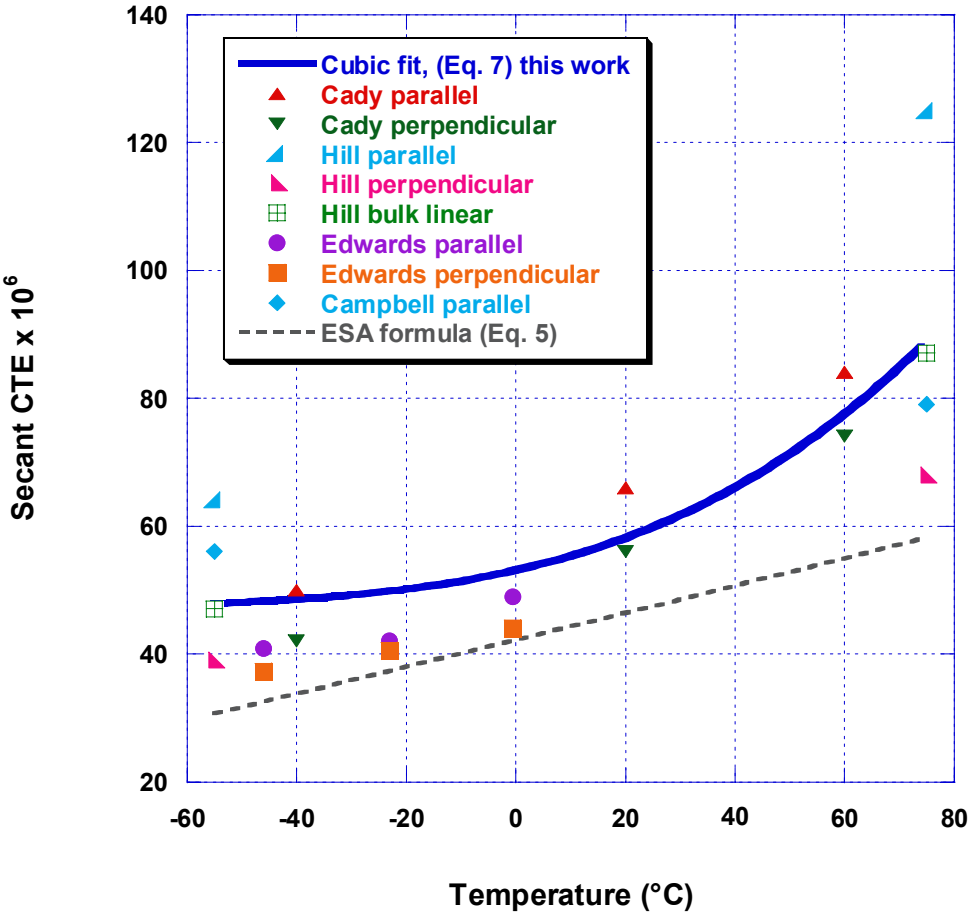

Fig. 10. Comparison of LANL secant CTE values for consolidated specimens of PBX 9502.

We note the consistent trend among Cady, Hill, and Edwards, who made the comparison that the parallel CTE is always greater than the perpendicular CTE. We note that our cubic fit lies below the parallel data reported by Cady (Ref. 14) and Hill (Ref. 21) and above their perpendicular data. We also note that the endpoints of our cubic fit match very closely with the bulk linear values reported by Hill. The three specimens we used for our final analysis included one with parallel orientation and two with perpendicular orientations. Among them, we observed no appreciable differences in CTE. For all these reasons, we believe that Eq. (7) represents bulk linear behavior.

3.0 Summary

With this report, we offer to the engineering community some level of phenomenological understanding and history associated with thermal expansion issues for PBX 9502. We have reported experimental difficulties in obtaining data and provided simple equations for calculating the bulk linear thermal expansion in an unconfined specimen of PBX 9502 consolidated to an average density of approximately 1.890 g/cm^3. We review our experience below.

Ninety cylindrical specimens were prepared for our investigation. This set included material from large cylindrical pressings and hemispherical stockpile returns. Parts with these geometries were consolidated from virgin PBX 9502 molding powder and from molding powder made with 50% recycled PBX 9502. Twenty specimens from a cylindrical mother derby composed of virgin molding powder were tested by measuring the change in length with temperature. The other 70 specimens have not been tested. With this report, we seek to provide a foundation for future testing.

Of the 20 tested, 11 specimens were heated in the first stage of taking measurements. We observed that this expansion was not reversible upon cooling, so we discounted all data collected after a specimen experienced the hot temperature extreme. We did not attempt to quantify the irreversible aspect of the growth. The expansion observed between the cold extreme and ambient temperatures was generally reversible. Therefore, we chose to focus our analysis on the nine specimens that were cooled first. Expansion data from one of these nine did not fully span the temperature range of interest and were not included in later analysis.

For each of the remaining eight specimens, we obtained a fit for the normalized displacement data. Curves representing instantaneous CTE data were obtained by calculating the derivative of the displacement fits. Some trends in those data were ambiguous, so we discounted the data from four specimens that had experienced operational problems with the initial run and had been re-tested. The data from those specimens were suspect because of their unknown thermal processing during the first tests, coupled with our knowledge of the irreversible growth manifested in the 11 heat-first specimens.

Of the four remaining specimens, the instantaneous CTE curves for three of them were very tightly grouped. We noted that the specimen with the outlying data came from the center of the mother derby, whereas the other three specimens came from the outer region and may

have been consolidated differently. Scrutiny of the density data also identified this specimen as an outlier. Therefore, we considered the outlying specimen to be of somewhat anomalous origin and did not include it in further analysis.

For our chosen three, we converted the instantaneous fits to secant CTE curves for which we calculated a single cubic fit with standard deviations in Eq. (7). We compared this fit to data from other LANL researchers and discovered that it represents bulk linear CTE values very well. We also discussed the proper application of our secant CTE fit in engineering calculations.

So, we began with ninety specimens and included data from only three in our final analysis for a variety of reasons. In spite of this incredible data attrition, we have enough confidence in our final result, Eq. (7), to recommend its use in calculating bulk linear CTEs for PBX 9502 pressed to nominal WR density. We believe that it will be useful in engineering calculations where thermal growth of PBX 9502 components may be of some consequence.

We were unable to obtain orientation-specific CTE values and we did not seek to measure or calculate volumetric CTE values. Thus, some CTEs in PBX 9502 remain elusive. We encourage further investigation, particularly for specimens from WR components and for specimens composed of 50% recycled PBX 9502.

4.0 References

1. John R. Kolb and H. F. Rizzo, "Growth of 1,3,5-Triamino-2,4,6-trinitrobenzene (TATB) I. Anisotropic Thermal Expansion," *Propellants and Explosives* **4**, 10–16 (1979).
2. B. H. Aubert, T. A. Butler, and J. C. Owen, "Chapter 7. Task 5: Load Path," in "Los Alamos National Laboratory's W80 6.2 SLEP Assessment Results (U)," Los Alamos National Laboratory document LA-CP-00-61 (SRD) (February 1, 2000), pp. 107–120.
3. Lawrence H. Van Vlack, *Elements of Materials Science and Engineering*, Fourth Ed. (Addison-Wesley, Reading, Massachusetts, 1980).
4. *Handbook of Chemistry and Physics*, 81st Edition (http://www.knovel.com/knovel2/default.jsp) (CRC Press, LLC, 2000).
5. Siegfried S. Hecker, "Plutonium and Its Alloys: From Atoms to Microstructure," in Challenges in Plutonium Science, *Los Alamos Science*, Volume II, LA-UR-00-4100 (2000), p. 263.
6. Howard H. Cady and Allen C. Larson, "The Crystal Structure of 1,3,5-Triamino-2,4,6-trinitrobenzene," *Acta Crystallographica* **18**, 485–496 (1965).
7. Bart Olinger and Howard Cady, "The Hydrostatic Compression of Explosives and Detonation Products to 10 GPa (100 kbars) and their Calculated Shock compression: Results for PETN, TATB, CO_2 and H_2O," *Sixth Symposium (International) on Detonation*, Colorado, California, August 24–27, 1976, pp. 700–709.

8. B. W. Olinger and Howard Cady, "Revised Thermodynamic Properties of Crystal Density TATB," Los Alamos Scientific Laboratory document M-6-264 (undated), pp. 91–93.

9. Howard H. Cady, "Microstructural Differences in TATB That Result From Manufacturing Techniques," *17th Annual Conference of ICT*, Karlsruhe, Germany, June 25–27, 1986, pp. 53-1 to 53-14.

10. Howard H. Cady, "Growth and Defects of Explosives Crystals," *Structure and Properties of Energetic Materials*, Boston, Massachusetts, November 30–December 2, 1992, pp. 243–254.

11. Harry F. Rizzo, James R. Humphrey, and John R. Kolb, "Growth of 1,3,5-Triamino-2,4,6-trinitrobenzene (TATB) II. Control of Growth by Use of High Tg Polymeric Binders," Lawrence Livermore Laboratory report UCRL-52662 (March 7, 1979).

12. Mark Rainbolt and Larry Hatler, "CTE Value for PBX 9502," Los Alamos National Laboratory memorandum ESA-WE-98-0422U to Brian Aubert (April 21, 1998).

13. Lyle E. Edwards, "Notebook data for CTE measurements on large pieces of PBX 9502 under P.O. 37858," Los Alamos National Laboratory, personal communication (February 22, 1977).

14. Howard H. Cady, Los Alamos National Laboratory, personal communication (August 3, 1998).

15. Jon L. Maienschein and F. Garcia, "Thermal Expansion of TATB-Based Explosives from 300 to 566 K," *Thermochimica Acta* **384**, 71–83 (2002).

16. Howard H. Cady, "WX-3 Monthly Report," Los Alamos Scientific Laboratory document WX-3-MR-75-4 (April 1975).

17. David S. Phillips, Los Alamos National Laboratory, personal communication (February 1999).

18. Roberta N. Mulford and Joseph A. Romero, "Sensitivity of the TATB-based Explosive PBX 9502 After Thermal Expansion," *Shock Compression of Condensed Matter*, Amherst, Massachusetts, July 27–August 1, 1997, pp. 723–726.

19. H. L. Flaugh, "CTE of PBX 9502," Los Alamos Scientific Laboratory memorandum to J. J. Ruminer (June 12, 1979).

20. A. W. Campbell, "Diameter Effect and Failure Diameter of a TATB-Based Explosive," *Propellants, Explosives, Pyrotechnics* **9**, 183–187 (1984).

21. L. G. Hill, J. B. Bdzil, and T. D. Aslam, "Front Curvature Rate Stick Measurements and Detonation Shock Dynamics Calibration for PBX 9502 Over a Wide Temperature Range," *Eleventh International Detonation Symposium*, Snowmass Village, Colorado, August 31 – September 4, 1998, pp. 1029–1037.

22. *ABAQUS Users Manual*, Version 5.8 (Hibbitt, Karlsson, and Sorenson, Inc., Providence, Rhode Island, 2000).

23. Mary Stinecipher Campbell, Danielle Garcia, and Deanne Idar, "Effects of Temperature and Pressure on the Glass Transitions of Plastic Bonded Explosives," *Thermochimica Acta* **(357–358)**, 89–95 (2000).

24. J. C. Dallman and J. Wackerle, "Temperature-Dependent Shock Initiation of TATB-based High Explosives," *Tenth International Detonation Symposium*, Boston, Massachusetts, July 12–16, 1993, pp. 130–138.

Los Alamos NM 87545